Fast Model Predictive Control of Sheet and Film Processes

Jeremy G. VanAntwerp and Richard D. Braatz, *Member, IEEE*

***Abstract*—Sheet and film processes are prevalent in the chemical and pulp and paper industries, and include paper coating, polymer film extrusion, and papermaking. A model predictive control algorithm is developed which is based on an off-line singular value decomposition of the plant. The input constraints are approximated by an ellipsoid whose size is optimized on-line to reduce conservatism. The controller has a structure proven to be robust to model inaccuracies and is computationally efficient enough for real-time implementation on large scale sheet and film processes (e.g., manipulated variable settings computed for 200 actuators in less than ten CPU seconds). The algorithm is applied to a paper machine model constructed from industrial data.**

***Index Terms*—Control systems, industrial control, large scale systems, model predictive control, optimal control, paper machine control, predictive control, process control.**

I. Introduction

SHEET and film processes are industrially important and include polymer film extrusion, papermaking, and paper coating. As detailed descriptions of sheet and film process control problems are available in the literature [1], [2], only their main characteristics are summarized here. Multivariable control of sheet and film processes is challenging due to: 1) large dimensionality; 2) model inaccuracies; and 3) actuator limitations [1]. The large-scale and high-speed nature of these processes place constraints on the amount of on-line computation available for the control algorithm, even with the processing speeds achievable by existing control hardware [3]. Process models for a sheet and film process have significant uncertainty associated with them, due to low signal-to-noise ratios, nonuniform shrinkage across the web, sideways movement of the entire web, and imprecise actuator movements. For any model-based controller, model uncertainty can significantly deteriorate closed-loop performance, and this is particularly true for sheet and film processes [4]. While being robust to this model uncertainty, the control algorithm must also avoid excessive actuator movements that may compromise the integrity of the actuating mechanism and the sheet/film.

In order to handle the process dimensionality within the computational constraints, existing industrial control algorithms for sheet and film processes are relatively simple. Typically, the sampling time for the control algorithm is chosen to be the time it takes the scanning sensor to make one or two complete scans across the sheet. Each scan consists of hundreds of individual sensor readings, which are typically grouped into blocks to reduce process dimensionality. Model inaccuracies are addressed through excessive detuning. This simplicity results in reduced product quality and a loss of flexibility.

Several methods have been proposed for designing controllers for sheet and film processes which are robust to model inaccuracies but do not directly address actuator limitations [5]–[7]. Model predictive control (MPC) approaches have been proposed that directly address actuator limitations [2], [3], [8], but do not explicitly address model inaccuracies. Also, these approaches require too much computation for implementation on large scale machines with much of the existing control hardware [3].

A method was recently proposed which [9] 1) directly addresses actuator limitations 2) has minimal on-line computational requirements; and 3) has a controller structure proven to be robust to model inaccuracies. The method was applicable to sheet and film processes in which all manipulated variable directions are controllable and the dynamics are adequately described by a pure time delay. As these assumptions do not always hold in practice, here we extend the method to handle singular plants with general dynamics. The resulting algorithm is applied to a paper machine model constructed from industrial data.

Note that, as is standard in the industrial control of sheet and film processes, this paper focuses on the control of profile properties across the web (in the literature this is called the cross-directional control problem [1]), since this is generally considered much more difficult than controlling a mean profile property. Readers interested in the latter problem including coupling to the cross-directional control problem are directed to the following papers and citations therein [1], [10]–[12].

II. Control Problem Statement

As is common in MPC, the process is represented by its finite impulse response

$$y(k+1) = y(k) + P\sum_{i=0}^{n_T} \beta_i u(k-i) \tag{1}$$

where

$u(k)$	vector of manipulated moves;
$y(k)$	sheet/film profile at time instance k;
P	interaction matrix (the mapping from inputs to outputs is assumed to be linear over the operating region which is a good assumption in practice).

Manuscript received April 1, 1998; revised June 3, 1999. Recommended by Associate Editor, F. Doyle. This work was supported by the DuPont Young Faculty Award, the UIUC Research Board, and the UIUC CSE program.

J. G. Van Antwerp is with Calvin College, Grand Rapids, MI 49506 USA.

R. D. Braatz is with the University of Illinois, Urbana-Champaign, Ulbana, IL 61801 USA.

Publisher Item Identifier S 1063-6536(00)03191-2.

The number of impulse response coefficients used to model the system is n_T and

$$\beta_i = g_{i+1} - g_i, \qquad \forall i = 0, \cdots, n_T \tag{2}$$

where g_i is the scalar such that $g_i P$ is the ith impulse response coefficient matrix, $\forall i = 1, \cdots, n_T$ and zero otherwise. This description can model a system with time delays by setting $\beta_i = 0, \forall i = 0, \cdots, \Theta$ where Θ is the time delay of the process. The interaction matrix P for a sheet and film process is typically nonsquare and singular or nearly singular [4], [13], [14].

The constraints on the manipulated variables form a finite polytope

$$u(k) \in \mathcal{P} \equiv \{u(k) | Au(k) \leq b\}. \tag{3}$$

For example, typical manipulated variable constraints for a sheet and film process are a minimum and maximum allowable value for each actuator [3], [9]

$$u_l \leq u(k) \leq u_h \tag{4}$$

and second-order bending constraints which limit the allowable differences between neighboring actuators

$$-l_b \leq Fu(k) \leq l_b \tag{5}$$

where

$$F = \begin{bmatrix} -1 & 1 & 0 & \cdots & \cdots & \cdots & 0 \\ 1 & -2 & 1 & \ddots & \ddots & \ddots & \vdots \\ 0 & 1 & -2 & \ddots & \ddots & \ddots & \vdots \\ \vdots & \ddots & \ddots & \ddots & \ddots & \ddots & \vdots \\ \vdots & \ddots & \ddots & \ddots & -2 & 1 & 0 \\ \vdots & \ddots & \ddots & \ddots & 1 & -2 & 1 \\ 0 & \cdots & \cdots & \cdots & 0 & 1 & -1 \end{bmatrix}. \tag{6}$$

The MPC problem is to compute $u(k)$ as the solution to the following quadratic program (QP):

$$\min_{u(k) \in \mathcal{P}} \sum_{j=1}^{p} [y(k+j) - r(k+j)]^T W_y [y(k+j) - r(k+j)] + [u(k) - u(k-1)]^T W_u [u(k) - u(k-1)] \tag{7}$$

$$\text{subject to} \qquad y(k+1) = y(k) + P \sum_{i=0}^{n_T} \beta_i u(k-i) \tag{8}$$

where $r(k+j)$ is the desired profile (which is usually flat), W_y and W_u are positive semidefinite weighting matrices, and p is the control horizon. Each weight (W_y, W_u) is assumed to be a constant multiplied by the identity matrix, which is appropriate for sheet and film processes. In particular, W_u is often selected large enough that rate constraints

$$-\Delta u_{\max} + u(k-1) \leq u(k) \leq \Delta u_{\max} + u(k-1) \tag{9}$$

are satisfied. Another method to handle rate constraints is described in [15].

The dynamics for sheet and film processes are simple enough that a control horizon of one is usually adequate, so for brevity this case is considered here. It is straightforward to generalize the control algorithm to handle larger control horizons (which would have increased computational requirements).

III. Fast MPC Control Algorithm

An overview of the proposed algorithm is presented in Table I. Only an outline of the algorithm derivation is given here. The complete derivation is given in [15]. The proposed control algorithm uses the singular value decomposition of the interaction matrix P

$$P = U \Lambda_P V^T \tag{10}$$

where Λ_P is a real $n_u \times n_u$ matrix whose diagonal elements are nonnegative, V is a real $n_u \times n_u$ orthogonal matrix (that is, $V^T V = I_{n_u}$), and U is the $n_y \times n_u$ matrix containing the left singular vectors of P where n_u is the number of elements of u, n_y is the number of elements of y, and I_n is the $n \times n$ identity matrix. The matrices Λ_P, U, and V are computed off-line using standard mathematical software. Due to strong interactions across the web, a number of the singular values of P will usually be zero or nearly zero [4].

The control algorithm approximates the finite polytope (3) with an ellipsoid

$$(u(k) - u_m)^T \Phi (u(k) - u_m) \leq \alpha \tag{11}$$

where u_m is the center and Φ defines the direction and relative length of the axes of an ellipsoid, and α is a scaling parameter which is optimized online to reduce conservatism (see below). The matrix Φ is selected to have the form

$$\Phi = V \Lambda_\Phi V^T \tag{12}$$

where Λ_Φ is a real, diagonal, positive definite matrix. Selecting Φ of the form in (12) fixes the directions of the axes of the ellipsoid (11) in n-dimensional space, and simplifies its off-line computation (see [15]).

By isolating the decision variables $u(k)$, a solution to (7) can be found very efficiently. The lone inequality constraint (11) introduces one Lagrange multiplier $\lambda > 0$. It can be shown that $h(\lambda)$ (defined in Table I) is monotonic in λ [15]. Consequently, $h(\lambda) = \alpha$ has a unique solution which is determined via bisection. This λ gives the $\hat{u}(k)$ which (suboptimally) solves the QP for a fixed scaling parameter α. The value of α is iterated until the resulting $\hat{u}(k)$ lies on the boundary of the polytope (3). Properties of the ellipsoid approximation [16] imply that α can be computed via bisection and will converge to a value

TABLE I
THE ROBUST ELLIPSOID (RE) ALGORITHM (ϵ_1 AND ϵ_2 ARE NUMERICAL TOLERANCES)

Offline	1. Compute and store the singular value decomposition of the process (10). 2. Compute and store an ellipsoid which is completely contained within the constraints (11). 3. Compute and store $D = W_u + \sum_{j=1}^{p} \gamma_j^2 {\Lambda_P}^T W_y \Lambda_P$.
Online	1. Obtain the current measurement $y(k)$. 2. Compute $N = W_u \hat{u}(k-1) - \Lambda_P U^T W_y \sum_{j=1}^{p} \gamma_j R_j(k)$. 3. Compute the unconstrained (transformed) actuator settings $\hat{u}_i^{\dagger}(k) = N_i / D_{ii}$. 4. Does $\hat{u}^{\dagger}$ satisfy the (transformed) polytopic constraints $AV\hat{u}(k) \le b$? If yes, GOTO 10, If no, continue. 5. BISECT on α 6. BISECT on λ 7. Compute $\hat{u}(k)$ from $[D + \lambda\Lambda_\Phi]_{ii}\,\hat{u}_i(k) = [\lambda\Lambda_\Phi \hat{u}_m + N]_i$. 8. Is $\lvert h(\lambda) - \alpha \rvert \le \epsilon_1$ (where $h(\lambda) \equiv \sum_{i=1}^{n_u} \Lambda_{\Phi,ii} (\hat{u}_i(k) - \hat{u}_{m,i})^2 = \sum_{i=1}^{n_u} \Lambda_{\Phi,ii} \left(\frac{(\lambda\Lambda_\Phi \hat{u}_m + N)_i}{(D + \lambda\Lambda_\Phi)_{ii}} - \hat{u}_{m,i} \right)^2 = \alpha$.)? If no, GOTO 6. If yes, continue. 9. Does (3) hold with $-\epsilon_2 \le \max_i \{[AV\hat{u}(k) - b]_i\} \le 0$? If no, GOTO 5. If yes, continue. 10. Implement the control action $u(k) = V\hat{u}(k)$. GOTO 1.

between one and $\alpha_{\max} = \hat{u}^{\dagger}(k)^T \hat{u}^{\dagger}(k)$. The exact value of α needed to produce a $\hat{u}(k)$ which lies on the boundary of the polytope is found via bisection. Since $\alpha = 1$ corresponds to an ellipsoid that is completely within the polytope, $\alpha = 1$ produces a $\hat{u}(k)$ which lies completely within the polytope. Likewise, $\alpha = \hat{u}^{\dagger}(k)^T \hat{u}^{\dagger}(k)$ produces a $\hat{u}(k)$ which lies outside the polytope [if $\hat{u}^{\dagger}(k)$ was within the polytope it would have been implemented—see Table I].

As the unconstrained solution approaches the manipulated variable constraint region, the performance of the proposed algorithm approaches that of the QP solution. Systems for which the unconstrained solution is regularly far outside the manipulated variable constraint set may have undersized actuators and/or a controller that is tuned too aggressively. In other words, the new algorithm will provide a good approximation to the QP for well-designed and well-tuned MPC control systems, but will provide a poorer approximation for poorly designed systems.

The actuator moves $u(k)$ to be implemented on the process are calculated from $u(k) = V\hat{u}(k)$ with the following exception. In practice, the experimental data used to construct the process model are not sufficiently informative to accurately identify many of the singular values and singular vectors in (10), [4], [13], [14]. These model errors can include time-varying phenomena including actuator stiction/backlash, nonuniform sheet shrinkage, variable transport delay, and varying process responses. Attempting the control these spatial modes will lead to very poor performance. The proposed algorithm is ideally suited to control only those singular vectors that are controllable. Since it uses the singular value decomposition of the plant, each $\hat{u}_i$ is independent and corresponds to a singular value of the process. Thus, if the singular value is known to be poorly captured by the process model (this can be determined using multivariable statistics [4], [13], [14]), then the corresponding $\hat{u}_i$ is simply set to zero.

The proposed algorithm requires no on-line calculations of matrix inverses, singular value decompositions, or determinants. The number of iterations [number of times $h(\lambda)$ is computed] for convergence is not a function of the size

$$R_j(k) = \begin{cases} y(k) - r(k+j) + U\Lambda_P \left[\sum_{i=1}^{j} \beta_i \left(\sum_{q=0}^{i-1} \hat{u}(k-i+q) \right) + \sum_{i=j+1}^{n_T} \beta_i \left(\sum_{q=0}^{j-1} \hat{u}(k-i+q) \right) \right], & j < n_T \\ y(k) - r(k+J) + U\Lambda_P \left[\sum_{i=1}^{n_T} \beta_i \left(\sum_{q=0}^{i-1} \hat{u}(k-i+q) \right) \right], & j \ge n_T \end{cases} \tag{13}$$

$$\gamma_j = \sum_{i=0}^{j-1} (j-i)\beta_i \quad j \le n_T \qquad \gamma_j = \sum_{i=0}^{n_T} (j-i)\beta_i \quad j > n_T \tag{14}$$

of the interaction matrix. The most computationally expensive steps in the algorithm for large n_u and n_y are the matrix multiplications required to translate between $(\hat{u}, y)$ and (u, y) coordinates. This is in contrast to the QP control algorithm (7) whose on-line computational expense is a higher order polynomial function of n_u, even for the fastest algorithms [17].

It is instructive to compare the robust ellipsoid (RE) algorithm with other "fast MPC" approaches. One strategy is to just compute the unconstrained control move, and then to "clip" each manipulated variable so that it satisfies the actuator constraints. While this algorithm is easy to implement, it

TABLE II
THE STRUCTURE OF THE INTERACTION MATRIX. THE VECTOR c IS SHOWN IN FIG. 1 AND WAS FIT FROM DATA IN [22, FIGS. 3 AND 5]

$$C = \begin{bmatrix}
c_2 & c_7 & c_{12} & \cdots & c_{37} & 0 & \cdots & \cdots & 0 & 0 \\
c_1 & c_6 & c_{11} & \cdots & c_{36} & 0 & \cdots & \cdots & 0 & 0 \\
c_0 & c_5 & c_{10} & \cdots & c_{35} & 0 & \cdots & \cdots & 0 & 0 \\
c_1 & c_4 & c_9 & \cdots & c_{34} & 0 & \cdots & \cdots & 0 & 0 \\
c_2 & c_3 & c_8 & \cdots & c_{33} & c_{38} & 0 & \cdots & 0 & 0 \\
c_3 & c_2 & c_7 & \cdots & c_{32} & c_{37} & 0 & \cdots & 0 & 0 \\
c_4 & c_1 & c_6 & \cdots & c_{31} & c_{36} & 0 & \cdots & 0 & 0 \\
c_5 & c_0 & c_5 & \cdots & c_{30} & c_{35} & 0 & \cdots & 0 & 0 \\
c_6 & c_1 & c_6 & \cdots & c_{29} & c_{34} & 0 & \cdots & 0 & 0 \\
c_7 & c_2 & c_7 & \cdots & c_{28} & c_{33} & c_{38} & \cdots & 0 & 0 \\
\vdots & \vdots & \vdots & \ddots & \vdots & \vdots & \vdots & \ddots & \vdots & \vdots \\
c_{35} & c_{30} & c_{25} & \cdots & c_0 & c_5 & c_{10} & \cdots & \vdots & \vdots \\
c_{36} & c_{31} & c_{26} & \cdots & c_1 & c_4 & c_9 & \cdots & \vdots & \vdots \\
c_{37} & c_{32} & c_{27} & \cdots & c_2 & c_3 & c_8 & \cdots & \vdots & \vdots \\
c_{38} & c_{33} & c_{28} & \cdots & c_3 & c_2 & c_7 & \cdots & \vdots & \vdots \\
0 & c_{34} & c_{29} & \cdots & c_4 & c_1 & c_6 & \cdots & \vdots & \vdots \\
0 & c_{35} & c_{30} & \cdots & c_5 & c_0 & c_5 & \cdots & \vdots & \vdots \\
\vdots & \vdots & \vdots & \ddots & \vdots & \vdots & \vdots & \ddots & \vdots & \vdots \\
\vdots & \vdots & \vdots & \cdots & \vdots & \vdots & \vdots & \cdots & c_2 & c_3 \\
\vdots & \vdots & \vdots & \cdots & \vdots & \vdots & \vdots & \cdots & c_3 & c_2 \\
\vdots & \vdots & \vdots & \cdots & \vdots & \vdots & \vdots & \cdots & c_4 & c_1 \\
\vdots & \vdots & \vdots & \cdots & \vdots & \vdots & \vdots & \cdots & c_5 & c_0 \\
\vdots & \vdots & \vdots & \cdots & \vdots & \vdots & \vdots & \cdots & c_6 & c_1 \\
0 & 0 & 0 & \cdots & 0 & 0 & 0 & \cdots & c_7 & c_2
\end{bmatrix}$$

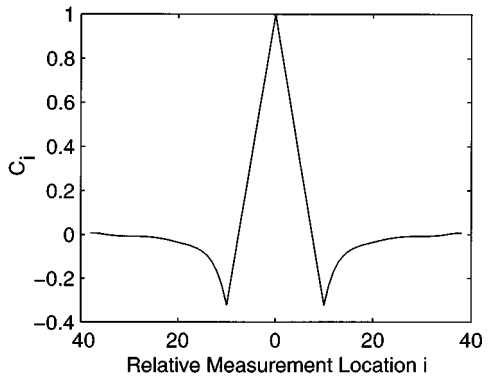

Fig. 1. The effect of a step change in one actuator on downstream measurements.

gives very poor closed-loop performance for ill-conditioned processes [18]. Standard ellipsoidal algorithms [19] and active set methods are slower than the best interior point algorithms [17], which require $O(n^3)$ flops to solve a QP, where n is the problem size [17]. The RE algorithm's most expensive step is a matrix-vector multiplication, which requires $O(n^2)$ flops. As will be seen in the paper machine example, this leads to a much faster control algorithm. The RE algorithm is also much faster than recently proposed customized linear program (LP)/QP algorithms [20], [21]. As such, it is the closest to achieving the 5-s sampling times which are enabled by the full-scanning technologies which are just now becoming available.

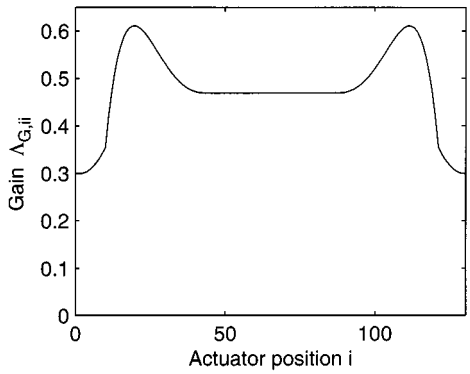

Fig. 2. Actuator gains as a function of position across the paper machine.

The RE algorithm is not a standard ellipsoidal algorithm [19], since Φ in (11) is computed only once. Standard ellipsoidal algorithms recompute a new ellipsoid that encloses the optimal solution at each step, which is at a higher computational cost relative to the RE algorithm which only *rescales* the ellipsoid at each step. The RE algorithm also has an intuitive motivation as the solution to an unconstrained QP with a time varying penalty on the vector of manipulated variables.

The transformation from an optimization problem over u to an optimization over $\hat{u}$ was motivated by results of Braatz *et al.* [5], [7], who showed that this decomposition corresponds to a controller structure that is robust to very general classes of perturbations in the plant interaction matrix. Furthermore, the control algorithm does not manipulate in directions that are uncontrollable due to model uncertainties. The inherent robustness of the RE algorithm will be demonstrated on a paper machine model constructed from industrial data.

IV. AN INDUSTRIAL PAPER MACHINE MODEL

In order to demonstrate the properties of the RE algorithm, a model was developed from industrial data that captures many of the realities of an industrial paper machine. Many of the features of this model are common to other sheet and film processes (e.g., constant interaction matrix, scalar dynamics, etc.). The model was developed from industrial identification data reported by Heaven *et al.* [22] who studied the slice lip to weight profile transfer function of a fine paper machine. The actuators are motors which change the slice lip openings and the weight profile is measured by a scanning sensor at the reel of the machine. Heaven *et al.*introduced pseudorandom binary sequences at a few different points across the machine and measured the downstream machine response (see [22] for details).

The model has the form

$$y(k+1) = y(k) + P[u(k-1) - (1-a_1)u(k-2) - a_1 u(k-3) + b_1 w(k)]. \quad (15)$$

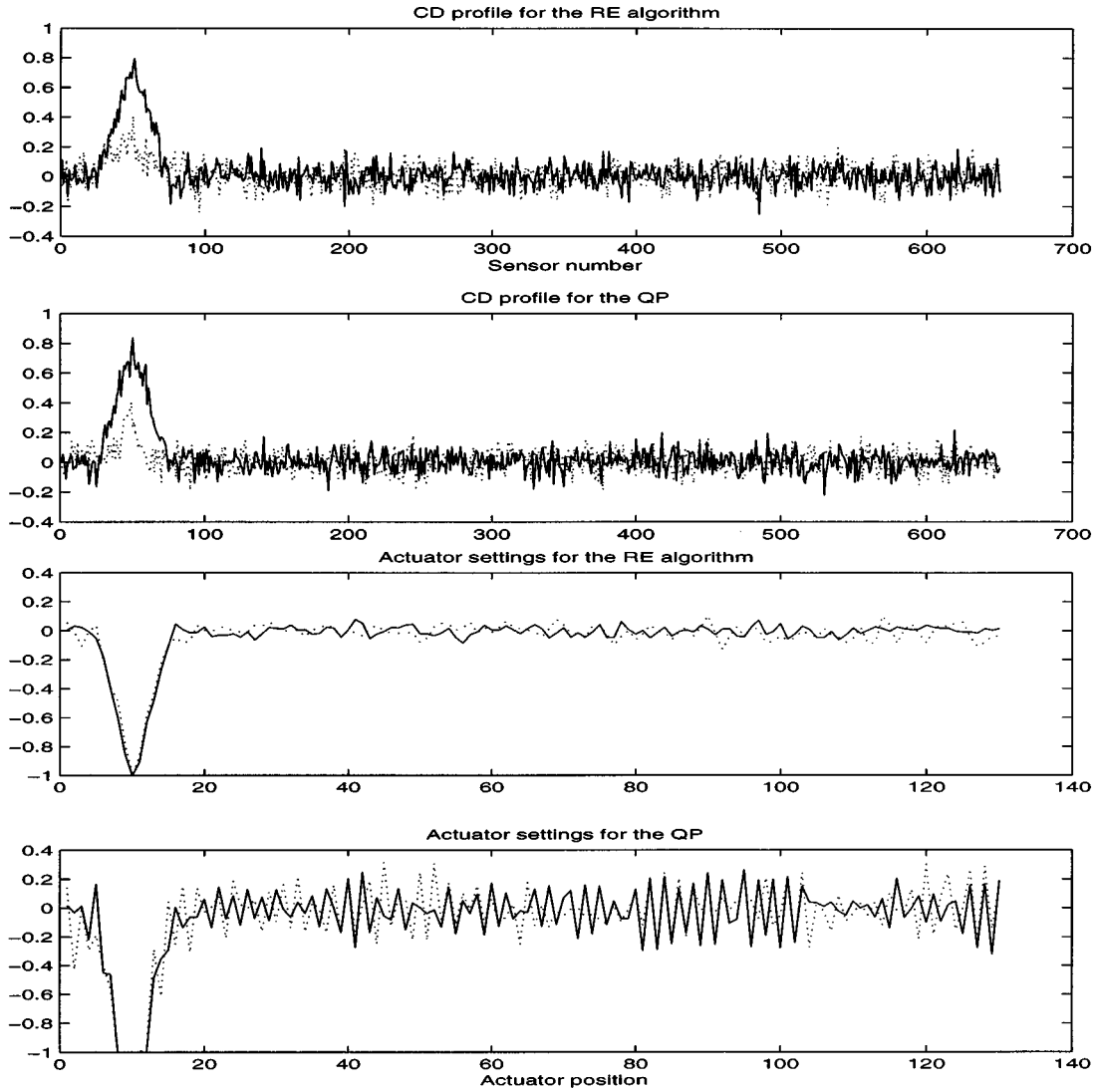

Fig. 3. Measurement profiles and manipulated variable settings are shown for the QP and RE algorithms when the web has an initial profile with a bump near the edge. The initial measurement profile is shown as a solid line, the steady-state profile is shown as a dotted line.

where

$y(k+1)$ vector of measurements of basis weight at time $k+1$;

$u(k-1)$ vector of actuator positions at time $k-1$;

P interaction matrix (with units of lbs/mil).

The vector $w(k)$ is a zero-mean Gaussian white noise signal that is integrated by the plant dynamics. This signal represents process disturbances and real paper machines are known to have disturbances of this sort (see, e.g., [22, eq. 3]). The magnitude of the disturbances $b_1 = 0.015$ was selected based on [22, Figs. 7 and 8]. The model structure with a time delay of 2 is taken from [22, eqs. 5 and 9] and $a_1 = 0.1533$ is reported in [22, Table 7]. Using the machine speed, Heaven *et al.* estimated the time delay as two full scans of the scanning sensor. It should be noted that for different machine speeds, the new time delay is easily estimated, but that the interaction matrix and model structure may change. The interaction matrix P represents the interactions between the 130 actuators and the 650 downstream measurement locations and is of the form

$$P = C\Lambda_G \tag{16}$$

where the matrix C is given in Table II.

Heaven *et al.* reported observing significantly different gains at the edges of the industrial paper machine but chose to average out these differences across the machine. On the other hand, we believe them to be an important feature of real paper machines. The diagonal matrix Λ_G captures the variation of the actuator gains across the machine as shown in Fig. 2. The $\Lambda_{G,ii}$'s were fit from data in [22, Table 2]. Analytic expressions for Λ_G and c are given in [15].

Reference [22, Fig. 7] shows constraints on the actuators of the form (4) with $u_l = -0.8$ and $u_h = 1.2$. For the model being

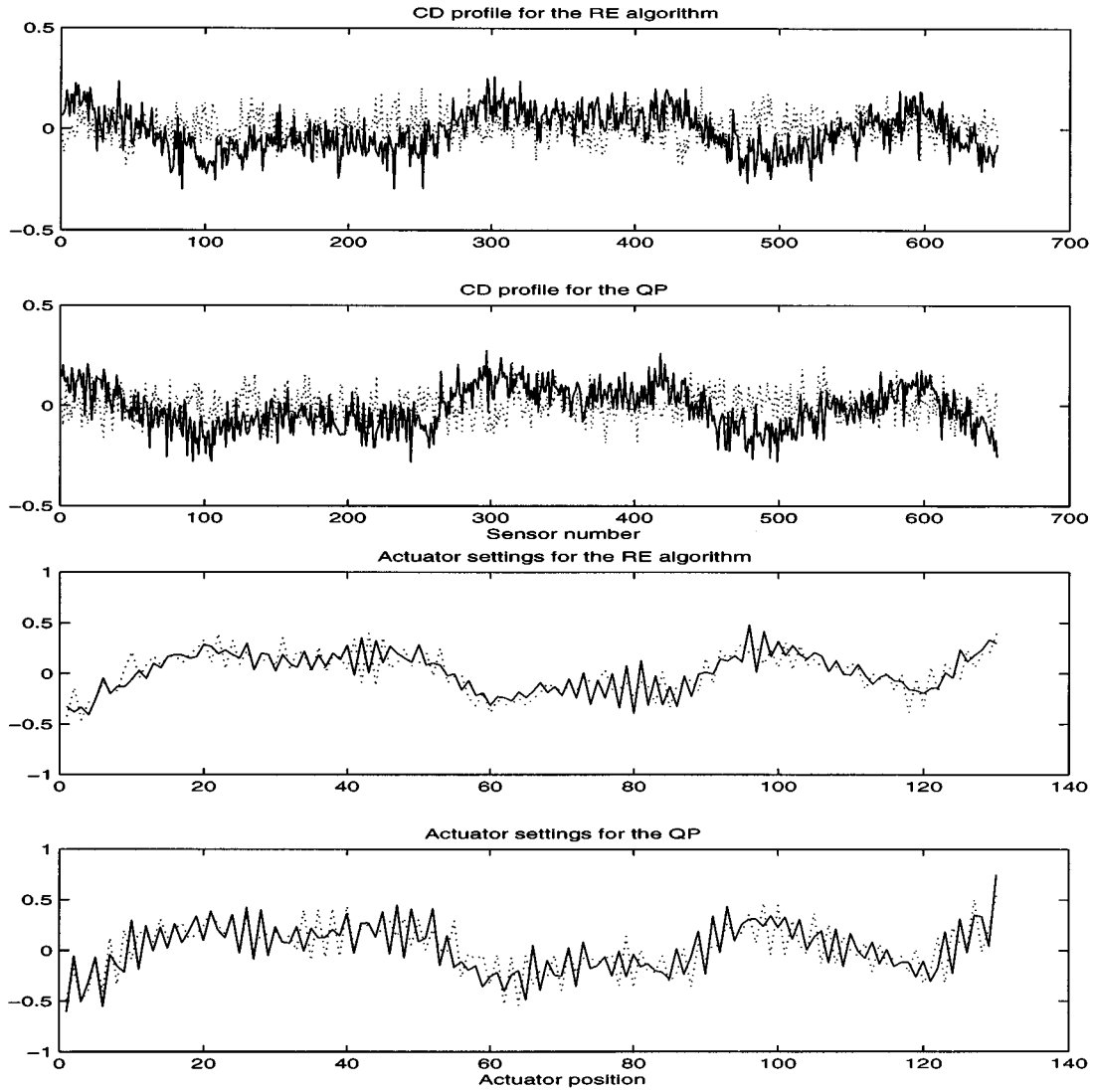

Fig. 4. Measurement profiles and manipulated variable settings are shown for the QP and RE algorithms when the web has a psuedorandom initial profile. The initial measurement profile is shown as a solid line, the steady-state profile is shown as a dotted line.

TABLE III
STEADY-STATE VARIANCES OF THE MEASURED PROFILE AND CPU TIME REQUIRED TO SOLVE THE PROBLEM ON A SPARC ULTRA 1 (143 MHz) WITH 64 MB OF RAM FOR THE THREE DIFFERENT INITIAL PROFILES. EACH NUMBER REPORTED HERE IS THE AVERAGE OF TEN SIMULATIONS TO AVERAGE OUT ANY EFFECTS OF THE RANDOM SEED (THE SECOND NUMBER IN EACH COLUMN IS THE SAMPLE STANDARD DEVIATION BASED ON 10 SIMULATIONS). ALTHOUGH NOT SHOWN HERE, THE PLOTS FOR THE CENTER BUMP DISTURBANCE ARE GIVEN IN [15]

$n_u = 130, n_y = 650$	side bump	center bump	pseudo-random profile
QP	2.042 ± 0.003	1.877 ± 0.003	1.840 ± 0.005
RE	2.102 ± 0.003	1.897 ± 0.002	1.838 ± 0.003
QP with plant model mismatch	3.274 ± 0.020	3.337 ± 0.009	3.224 ± 0.043
RE with plant model mismatch	2.150 ± 0.008	1.913 ± 0.003	1.836 ± 0.004

developed here, these constraints will be recentered ($-u_l = u_h = 1$). Additionally, we will impose constraints of the form (5) with $l_b = 1$, as constraints of this type are usually specified for real paper machines [3].

The measurement is subject to noise

$$y_{meas}(k) = y(k) + b_2 v(k) \tag{17}$$

where $y(k)$ is given by (15) and $v(k)$ is a vector of zero-mean Gaussian white noise chosen to be representative of the data ob-

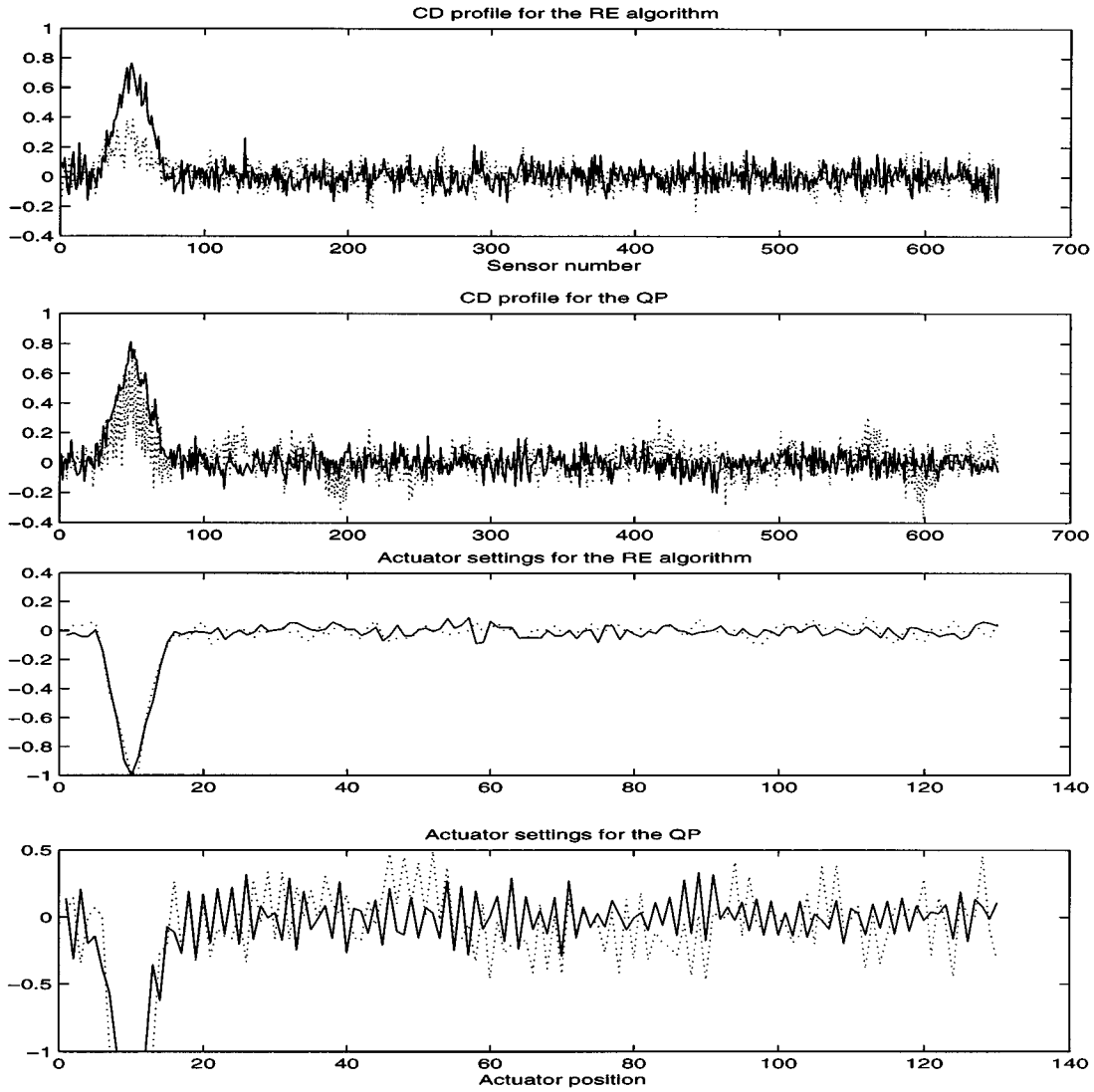

Fig. 5. Measurement profiles and manipulated variable settings are shown for the QP and RE algorithms when the plant is misidentified. The initial measurement profile is shown as a solid line, the steady-state profile is shown as a dotted line.

tained from a real paper machine (e.g., [22, eq. 3]). The magnitude of the noise b_2 was chosen to be equal to 0.067 in order to match the level of noise in [22, Figs. 7 and 8].

This same model form will also used for a process with more sensors and actuators by interpolating the vector of interaction parameters c and the gains across the machine Λ_G. This corresponds to a paper machine where the actuators and measurements are spaced more closely, rather than a wider machine with the same actuator spacing. The motivation for scaling the control problem in this way is that paper machines are unlikely to become significantly wider in the near future, but there is likely to be a continued increase in the number of actuators and sensors.

V. Simulation Results and Discussion

The RE algorithm was compared to traditional MPC on the paper machine model. The traditional MPC formulation results in a constrained QP with n_u decision variables. This QP was solved using IMSL's QP solver, which is implemented in FORTRAN. For the closed-loop simulations shown here, the controller tuning parameters, W_y and W_u, were chosen to be $2I$ and $0.01I$ and ϵ_1 and ϵ_2 were chosen to be 10^{-6} and 2×10^{-6}, respectively. The control horizon was $p = 10$.

The closed-loop performance of the RE and traditional MPC algorithms were tested on the paper machine model with three different initial measured profiles; one with a bump near the edge, one with a bump near the center, and a pseudorandom profile. For the case of no plant/model mismatch, the RE and QP algorithms achieve similar measured profiles (see Figs. 3 and 4 and Table III), but the RE algorithm has a much smoother series of input vectors (see Figs. 3 and 4), which produces less stress on the slice lip.

As discussed in the control algorithm section, many of the smaller singular values are poorly identified in practice. The corresponding singular vectors are also poorly known, and in fact, even their general direction cannot be predicted with confidence from the experimental data [4], [13], [14]. Attempting to

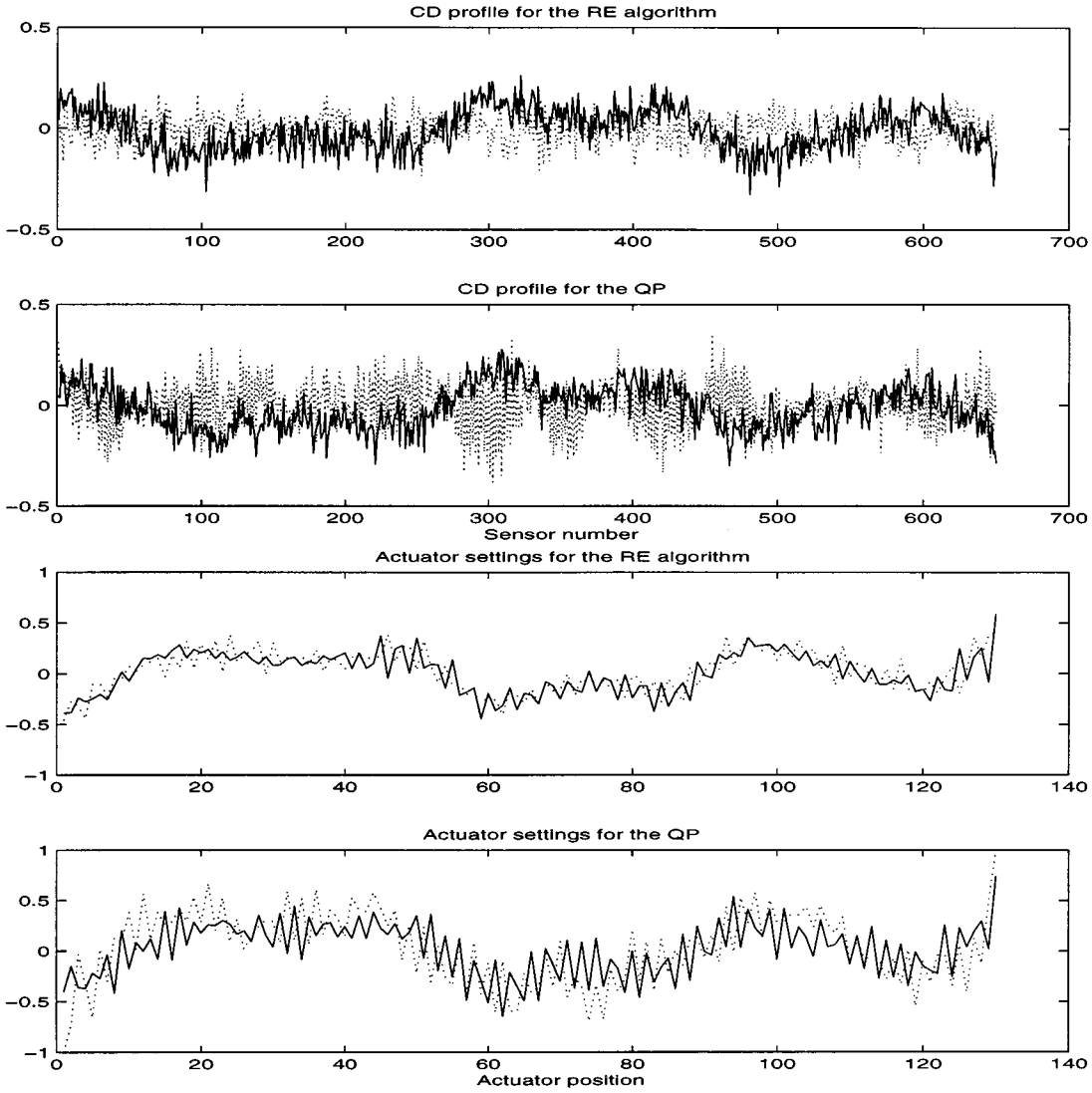

Fig. 6. Measurement profiles and manipulated variable settings are shown for the QP and RE algorithms when the plant is misidentified. The initial measurement profile is shown as a solid line, the steady-state profile is shown as a dotted line.

manipulate in these directions will result in poor performance. Featherstone and Braatz [13], [14] give algorithms for quantifying and minimizing the error in the singular values with statistical confidence during model identification.

To compare the robustness of the two algorithms to plant/model mismatch, the directions of the singular vectors in U were flipped for $i = 113, 116, 117, 118, 119, 121, 126, 127, 129,$ and 130. This new plant $\hat{P}$ will be assumed to be the true process. For each controller, the manipulated variable vector was calculated based on P but was implemented on $\hat{P}$. Featherstone and Braatz [13] give criteria for deciding which singular values should be controlled and which should not. For this study, we will assume that the 20 smallest singular values were determined to be uncontrollable. For the RE algorithm, $\hat{u}_i$ was set equal to zero for $i = 111, \cdots, 130$. Thus, the RE algorithm is controlling the paper machine based on the reduced order controllable portion of the model. The misidentified plant results in poor performance for the QP, but the performance of the RE algorithm suffers only slightly (see Figs. 5 and 6 and Table III). Also, the jaggedness of the QP manipulated variable vectors becomes more pronounced while the RE manipulated variable vectors are virtually the same (see Figs. 5 and 6).

Fig. 7 shows how the computation time for the RE and QP algorithms grows as a function of the number of actuators. The slope of each line is an estimate of the rate of growth of the solution time as a function of the problem size (e.g., a slope of 3 means the solution time grows as n_u^3). The computation time for the RE algorithm grows more slowly as a function of n_u than the time required by the QP. The RE algorithm is fast enough to be implemented on real paper machines, even those of very high dimensionality, while providing robustness to model uncertainties (e.g., manipulated variable settings for 200 actuators in under ten CPU s).

A few final comments are in order. The MPC algorithm could be modified to not manipulate in uncontrollable plant

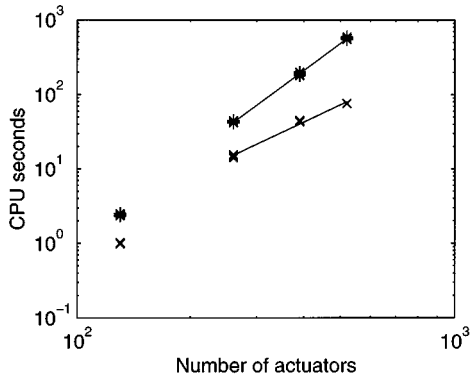

Fig. 7. The CPU time for the QP (*) and RE (x) algorithms are shown as a function of the number of actuators. For each algorithm, for each number of actuators, the solution time for ten different random seeds is shown. The slopes of the lines shown are 3.73 for the QP and 2.38 for the RE algorithm. The optimizations were run on a Sparc Ultra 1 workstation (143 MHz) with 64 MB of RAM.

directions [13]. Still, the RE algorithm is faster, and has the robust optimal controller structure for a wide variety of model uncertainty structures [7]. Also, not manipulating in the uncontrollable directions arises very naturally with the RE algorithm. The simulation results for the paper machine considered here, and other results for a polymer film extruder considered elsewhere, suggestthat constraint handling is actually unnecessary for some (but not all) web processes, provided that the control algorithm does not attempt to manipulate in uncontrollable directions of the process [4]. This is because manipulated variable moves in the controllable plant directions (which correspond to the larger singular values) have a strong effect on the plant output. In cases where constraint handling is needed, the RE algorithm can quickly compute a feasible control move.

VI. Conclusions

An algorithm for the control of sheet and film processes has been developed which directly addresses actuator limitations and model uncertainties. The algorithm is based on an off-line singular value decomposition of the plant. The polytopic manipulated variable constraints are approximated with an ellipsoid whose size is optimized on-line to reduce conservatism. The control algorithm only manipulates in controllable plant directions, which are identified using cited statistical criteria.

A model of a fine paper machine was constructed from industrial identification data. The model captures more of the realities of paper machine operations than other models reported in the literature. In the case where there was no plant/model mismatch, the robust ellipsoid algorithm provided similar closed-loop profile responses as classical model predictive control, but with much smoother manipulated variable profiles. In the practical case where there were model uncertainties, the robust ellipsoid algorithm provided substantially reduced profile variability. The robust ellipsoid algorithm was also substantially faster than classical quadratic programming-based model predictive control—an order of magnitude faster for the paper machine with 520 actuators. The robust ellipsoid algorithm is sufficiently computationally efficient to be implemented in real time on large scale sheet and film processes.

References

[1] R. D. Braatz, B. A. Ogunnaike, and A. P. Featherstone, "Identification, estimation, and control of sheet and film processes," in *Proc. IFAC World Congr.*. Tarrytown, NY, 1996, pp. 319–324.
[2] J. B. Rawlings and I.-L. Chien, "Gage control of film and sheet-forming process," *AIChE J.*, vol. 42, pp. 753–766, 1996.
[3] S.-C. Chen and R. G. Wilhelm Jr., "Optimal control of cross-machine direction web profile with constraints on the control effort," in *Proc. Amer. Contr. Conf*. Piscataway, NJ, 1986, pp. 1409–1415.
[4] A. P. Featherstone and R. D. Braatz, "Control-oriented modeling of sheet and film processes," *AIChE J.*, vol. 43, pp. 1989–2001, 1997.
[5] M. Hovd, R. D. Braatz, and S. Skogestad, "SVD controllers for H_2-, H_∞-, and μ-optimal control," *Automatica*, pp. 433–439, 1996.
[6] D. Laughlin, M. Morari, and R. D. Braatz, "Robust performance of cross-directional basis-weight control in paper machines," *Automatica*, vol. 29, pp. 1395–1410, 1993.
[7] R. D. Braatz and J. G. VanAntwerp, "Robust cross-directional control of large scale paper machines," in *Proc. IEEE Int. Conf. Contr. Applicat*. Piscataway, NJ, 1996, pp. 155–160.
[8] T. J. Boyle, "Control of cross-direction variations in web forming machines," *Canada J. Chem. Eng.*, vol. 55, pp. 457–461, 1977.
[9] R. D. Braatz and J. G. VanAntwerp, "Advanced cross-directional control," *Pulp Paper Canada*, vol. 98, no. 7, pp. T237–T239, July 1997.
[10] L. G. Bergh and J. F. MacGregor, "Spatial control of sheet and film forming processes," *Canada J. Chem. Eng.*, vol. 65, pp. 148–155, 1987.
[11] R. D. Braatz, M. L. Tyler, M. Morari, F. R. Pranckh, and L. Sartor, "Identification and cross-directional control of coating processes," *AIChE J.*, vol. 38, pp. 1329–1339, 1992.
[12] A. Rigopoulos, Y. Arkun, F. Kayihan, and E. Hanczyc, "Estimation of paper machine full profile properties using Kalman filtering and recursive principal component analysis," in *Proc. 5th Int. Conf. Chem. Process Contr. (CPC-V)*, Tahoe City, CA, 1996.
[13] A. P. Featherstone and R. D. Braatz, "Integrated robust identification and control of large scale processes," *Ind. Eng. Chem. Res.*, vol. 37, pp. 97–106, 1998.
[14] ——, "Input design for large scale sheet and film processes," *Ind. Eng. Chem. Res.*, vol. 37, pp. 449–454, 1998.
[15] J. G. VanAntwerp and R. D. Braatz, "Fast model predictive control of sheet and film processes," Univ. Illinois, Urbana, IL, LSSRL Tech. Memo UIUC-LSSRL 99-001.
[16] L. G. Khachiyan and M. J. Todd, "On the complexity of approximating the maximal inscribed ellipsoid for a polytope," *Math. Prog.*, vol. 61, pp. 137–159, 1993.
[17] Y. Nesterov and A. Nemirovskii, *Interior Point Polynomial Algorithms in Convex Programming*. Philadelphia, PA: SIAM, 1994, vol. 13, Studies in Applied Mathematics.
[18] P. J. Campo and M. Morari, "Achievable closed-loop properties of systems under decentralized control: Conditions involving the steady-state gain," *IEEE Trans. Automat. Contr.*, vol. 39, pp. 932–943, 1994.
[19] R. G. Bland, D. Goldfarb, and M. J. Todd, "The ellipsoid method: A survey," *Operations Res.*, vol. 29, pp. 1039–1091, 1981.
[20] P. Dave, J. Pekny, and F. Doyle, "Customization strategies for the solution of linear programming problems arising from large-scale model predictive control of a paper machine," Purdue Univ., School Chem. Eng., West Lafayette, IN, CIPAC Tech. Rep., 1997.
[21] C. V. Rao, J. C. Campbell, J. B. Rawlings, and S. J. Wright, "Efficient implementation of model predictive control for sheet and film forming processes," in *Proc. Amer. Contr. Conf*. Piscataway, NJ, 1997, pp. 2940–2944.
[22] E. M. Heaven, T. M. Kean, I. M. Jonsson, M. A. Manness, K. M. Vu, and R. N. Vyse, "Applications of system identification to paper machine model development and controller design," in *2nd IEEE Conf. Contr. Applicat.*, Vancouver, BC, Canada, Sept. 13–16, 1993, pp. 227–233.

Jeremy G. VanAntwerp received the B.S. degree in chemical engineering with high honor from Michigan State University, East Lansing, in 1994. He received the M.S. and Ph.D. degrees in chemical engineering from the University of Illinois at Urbana-Champaign in 1997 and 1999, respectively.

He is currently an Assistant Professor of Engineering at Calvin College, Grand Rapids, MI. His research interests include robust nonlinear control, optimal experimental design, paper machine control, and bilinear matrix inequalities.

In 1995, Dr. VanAntwerp received a Computational Science and Engineering Fellowship which supported his development of an algorithm for solving optimizations over bilinear matrix inequalities, which he applied to several processes including reactor networks, reactive ion etching, and paper machines.

Richard D. Braatz (M'96) received the B.S. degree in chemical engineering from Oregon State University, Corvallis, in 1988 and the M.S. and Ph.D. degrees in chemical engineering from the California Institute of Technology, Pasadena, in 1991 and 1993, respectively.

After a postdoctoral year at DuPont, he joined the faculty at the University of Illinois, Urbana-Champaign, in 1994 as an Assistant Professor. Since 1997, he has also held joint positions with the National Center for Supercomputing Applications and the Computational Science and Engineering Program. His research interests include large scale systems theory and applications, multidimensional crystallization, bilinear matrix inequalities, and robust nonlinear control.

Dr. Braatz was awarded the Hertz Doctoral Thesis Prize in 1993, the DuPont Young Faculty Award in 1995, and the Xerox Award for Faculty Research in 1999.